Journal of Building Engineering 107 (2025) 112445

Contents lists available at ScienceDirect

Journal of Building Engineering

journal homepage: www.elsevier.com/locate/jobe

Robust model predictive control of battery energy storage with neural network forecasting for peak shaving in university campus

Nicolas Mary *, Louis-A. Dessaint

Electrical Engineering Department, École de Technologie Supérieure, Montreal, QC, H3C 1K3, Canada

ARTICLE INFO

Keywords:
Artificial neural networks
Battery
Buildings
Peak demand management
Peak shaving
Predictive control
Robust optimization

ABSTRACT

This study addresses the challenge of optimizing energy consumption and managing peak demand charges in large university campuses using battery energy storage system (BESS) by demonstrating the effectiveness of a two-stage neural network-based Model Predictive Control (MPC) algorithm enhanced with robust optimization. To achieve this, we first delineate the architecture of neural networks and the Robust MPC model. Subsequent testing in simulation environments leads to the practical validation of the algorithm on a small-scale test bench configured to emulate a microgrid system. Results show that the integration of neural networks and robust optimization in an MPC framework significantly outperforms traditional control methods, achieving more effective peak shaving, reducing energy costs, and enhancing system resilience. The added robustness effectively addresses forecasting errors, making the control strategy more resilient and reliable. The successful deployment of this algorithm on a test bench underscores its practical applicability, highlighting its potential to optimize energy consumption and reduce peak demand charges in buildings. This research contributes a novel, scalable, and adaptive control strategy that bridges advanced forecasting techniques with robust MPC, providing a valuable solution to address peak demand challenges in commercial and institutional buildings.

1. Introduction

Efficient management of peak demand is crucial for utility companies, given the constraints in power generation capacities and the limitations of the distribution networks. During periods of extreme temperatures, such as especially cold or hot days, utilities face significant challenges. To ensure a continuous electricity supply to their consumers, they must often rely on cost-intensive and environmentally detrimental energy sources like natural gas or coal-fired plants [1].

To reduce the impact of peak power demand on the electricity grid, utilities usually bill power demand based on the highest level attained during a specified time range (e.g., a month). Utilities set a predetermined limit known as the contract power, which is billed regardless of whether a building reaches this threshold. However, should the power usage surpass the contract power, the power portion of the electricity bill usually increases.

This billing mechanism incentivizes large building owners to keep their power usage at or below the contract power level. A way to reduce peak power is fuel-switching during high demand periods. For example, using natural gas instead of electricity. However, in regions where electricity is both cost-effective and environmentally friendly, such as areas with hydroelectricity-based grids, this method is rarely advantageous from neither an economic nor environmental standpoint. An exception is made where conjoint program

* Corresponding author.
E-mail address: nicolas.mary.2@ens.etsmtl.ca (N. Mary).

https://doi.org/10.1016/j.jobe.2025.112445
Received 18 November 2024; Received in revised form 28 January 2025; Accepted 19 March 2025
Available online 11 April 2025
2352-7102/© 2025 The Authors. Published by Elsevier Ltd. This is an open access article under the CC BY-NC-ND license (http://creativecommons.org/licenses/by-nc-nd/4.0/).

between gas and electricity utilities exists [2]. Therefore, the primary strategy for lowering energy expenses, aside from decreasing total energy consumption, involves minimizing the building's power demand through peak shaving [3]. Peak shaving is not inherently an energy efficiency measure, as it does not reduce the total electricity consumption of a building. Rather, it is a demand management strategy aimed at optimizing both the timing and magnitude of electricity usage [3].

Different strategies exist to perform peak shaving [4]. The first major one consists in modifying the load profile of the building to level the energy consumption throughout the day. For example, cascading the starting time of operation of heating and ventilation systems. Often called demand management or load levelling, this method can be highly efficient but necessitates a deep analysis and modification of the building consumption pattern which are often tightly linked to the inhabitant's habits or to industrial processes [5–7]. Another approach, which this paper focuses on, involves using distributed energy resources to power the building during peak demand. This way, the building stays within the contracted power limits from the utility standpoint, and no changes are necessary to the building's consumption pattern [4]. This approach requires a controllable electricity source with high availability and low operational cost such as battery-based energy storage system (BESS). BESS are highly reliable, have quick response time and do not rely on fossil fuel. However, BESS are costly and have a relatively short lifespan [8]. As a result, their installation in a large building requires precise optimization of the BESS capacity and power characteristics along with advanced control mechanisms [4,9]. Indeed, performing peak shaving in a large building using a BESS presents several challenges to which we propose solutions in this article.

The first challenge in performing peak shaving arises from the way peak demand is usually calculated, which is based on the highest power level reached during any 15-min interval within the billing cycle. The control system must consistently manage peak shaving throughout the entire period, as failing to mitigate even a single peak can undermine all prior efforts for that billing cycle. The second challenge arises from the diversity of periods at which power peaks can happen. Especially with large commercial, institutional or industrial buildings, it is uneasy to find a generic discharge pattern for the batteries because several peaks of varying amplitudes can happen throughout the day. Yet, it is impossible for the BESS to follow the load and discharge whenever a peak occurs as it would require a very large capacity BESS whose high cost would render non-economically viable. Thus, to perform peak shaving without installing such a system, building load predictions are usually performed, and optimization is run using these predictions to make the most out of the power and capacity available from a smaller BESS.

Performing peak load shaving using a BESS has been intensively covered in the literature along with the impact of forecasting errors on its efficiency [4,10,11].

Several forecasting methods have been used in the literature such as Support Vector Machine [12], random noise applied on historical data [13,14] or artificial neural networks (ANN) [10,15–18]. In Ref. [15], the authors successfully forecast a university campus load using ANN and obtain a mean average percentage of error of approximately 5 %. However, this error is usually higher in periods of power peaks when accuracy is the most critical. Due to the first aforementioned challenge, it is critical that the forecasting errors are considered when optimizing the BESS charging and discharging schedule.

Methods exist to handle such uncertainties in the forecasts such as fuzzy logic [19], robust optimization (RO) [20] or the model predictive control (MPC) approach. The latter has proven to be efficient in Refs. [12–15,18–21] as it is based on a receding finite-time horizon over which the optimization is carried out at fixed intervals. It enables updating the forecasted values to gain accuracy and taking real-time information, such as BESS state-of-charge (SOC), as input of the optimization process. Usually, the MPC approaches use a model of the system to forecast its future states. However, it can also be used conjointly with other means of forecasting as seen in Ref. [18]. One limitation of the model predictive control approach lies in the fact that it does not explicitly consider the forecasting error but rather corrects itself throughout the day. Thus, if a bad decision is made early in the day, the peak shaving effort could fail.

To palliate this limitation, we propose the use of robust optimization which has become a method of choice for optimization problems under uncertainty in power systems engineering. [22–24]. Its objective is to devise solutions that remain effective under various uncertain conditions, ensuring that the outcomes are not overly sensitive to changes in the input data or assumptions. In other words, it usually considers the worst-case scenario then acts according to it to ensure robustness of the proposed solution. One limitation of such an optimization process is that it can be overly conservative [25], which in this case is a risk worth taking to avoid negating all efforts made during a month with one daily missed peak.

In this article, we propose a novel two-stage robust MPC approach using neural networks forecasting to perform peak shaving on large university campus buildings using BESS. The originality of the proposed work relies on the combination of neural networks and Robust MPC using a budget of uncertainty to perform peak shaving and on its implementation in a real-life setting enabling for validation of its applicability. The output of the optimization process (also called the asynchronous layer) is not directly a schedule of the BESS power for the entire day, as often seen in the literature. Instead, it outputs the peak shaving limit at which the Energy Management System (EMS) calculated it can shave the load for the entire day. This limit, called setpoint, is then used by the synchronous, real-time layer of the controller that compares real load demand to the peak shaving limit to compute the power of the BESS. This process ensures that only the exact amount of energy is used to shave the load demand to the desired limit thus conserving energy stored for the rest of the day. More importantly, the use of robust optimization with a budget of uncertainty within a two-stage neural-network-based MPC framework to perform peak shaving using BESS constitutes the main contribution. Indeed, in Ref. [26] authors used a robust MPC framework on a large-scale park microgrid to control chillers and perform peak shaving while adhering to temperature constraints. Also, in Ref. [27] authors used a robust MPC framework to control all assets inside a large microgrid. However, none of those papers presented the use of neural networks to perform their predictions. Moreover, they did not validate the applicability of their methods. In fact, only few authors found in the literature [12,21,28] present an experimental validation of their results which is what is proposed on this article thanks to a small-scale microgrid system.

This study aims to evaluate both theoretically and experimentally the effectiveness of a two-stage neural network-based control system for BESS to perform peak shaving. The system integrates robust optimization with a budget of uncertainty within a model

predictive control (MPC) framework to address and mitigate forecasting errors. Its primary function is to perform peak shaving in large university campus with versatile load profiles with residential, commercial, and institutional characteristics.

The proposed system seeks to minimize operational costs of buildings by reducing electricity bills for the end users. Additionally, it supports utility companies by contributing to a stable and cleaner energy supply for their customers, including the building where peak shaving is implemented.

2. Methodology

2.1. Load forecasting using neural networks

As previously explained in section 1, it is essential to forecast the load demand to optimize the charging and discharging schedule of a BESS performing peak load shaving. Neural networks are proposed for these predictions. The architecture of the different neural networks (NN) used has been defined in previous paper [15,29] and will only be summarized in present paper.

The forecasting layer comprises two deep feedforward neural networks, each with four fully connected hidden layers containing 25 neurons per layer. The Rectified Linear Unit activation function was used, and training was conducted using the Adam optimization algorithm. Both NNs were continuously trained on historical data with a 5-min resolution from January 2017 to December 2022, excluding 2020 due to the Covid-19 pandemic which significantly disrupted load demand patterns.

Once trained, the neural networks operate in real time to forecast the building's load demand for the current day, spanning from the present time to the end of the day. The 24-h-ahead (24HA) network predicts one quarter-hour interval using a vector of 8 input variables and processes 96 such vectors to cover the entire day. In contrast, the 2-h-ahead (2HA) network uses a 20-variable input vector to generate 8 outputs, each corresponding to a quarter-hour interval within the 2-h forecasted window.

Input data for both networks includes time-dependent variables (current date and time and day of the week), meteorological data (outdoor temperature), and historical load power and energy consumption, all of which have been shown to significantly impact building load behavior [15]. The combined output of both neural networks provides forecasted mean load power (in kW) at 15-min intervals for the next 24 h.

2.2. Non-robust optimization model formulation

A linearized mixed integer linear programming optimization model has been defined to compute the optimal power setpoint that the building energy management system (EMS) must follow to reduce the building peak power demand and consequently, its energy bills.

First, we define a minimization problem, *f,* where the objective function (1.1) minimizes the utility bill by accounting for time-of-use energy costs and power costs, while also incorporating a constraint to maintain a sufficient level of charge in the BESS. This approach helps ensure its availability for unexpected events.

$$\begin{aligned}\min f = &\left[\sum_{t=0}^{N-1} \left(P_l(t) - P_b\,(t)\right) \cdot \Delta t \cdot C_e(t)\right] \\ &+\left[\sum_{t=0}^{N-1} \lambda_{ch} \cdot \left(1 - \left(\frac{E_b(t) + \Delta E_b(t)}{B_{cap}}\right)\right)\right] \\ &+\left[P_{p,m} \cdot\ C_p\right]\ (\forall t \in T_m, \forall m \in M)\end{aligned} \tag{1.1}$$

In the first term, which represents the energy part of the bill, $P_l(t)$ is the building load power at time t in kW, $P_b(t)$ the BESS power at time t in kW, Δt the time step duration in hours and $C_e(t)$ the cost of energy at time t in \$/kWh. In the second term, ensuring the BESS is maintained at a sufficient level of charge, λ_{ch} is a fee applied to the available energy in the BESS in \$/kWh, $E_b(t)$ is the available energy in the BESS at time t, $\Delta E_b(t)$ is the variation of the energy available in the BESS during the entire duration Δt which starts at time t and B_{cap} is the effective capacity of the BESS in kWh. In the last term, representing the power part of the bill. The variable $P_{p,m}$ is the maximum power peak of the current month m in kW and C_p the cost of power in \$/kW. Finally, M is a natural number set with index m of size twelve corresponding to each month in a Gregorian year and T_m is a non-negative integer set with index t of size N that will vary according to the number of days in the month m and the resolution of the used data. T_m corresponds to all the time steps constituting an entire month.

BESS power is subject to constraints (2.1) to (2.3)

$$P_b(t) = P_b^{dis}(t) - P_b^{ch}(t)\ (\forall t \in T_m) \tag{2.1}$$

$$0 \le P_b^{ch}(t) \le P_b^{max} \cdot\ y_{ch}(t)\ (\forall t \in T_m) \tag{2.2}$$

$$0 \le P_b^{dis}(t) \le P_b^{max} \cdot\ (1 - y_{ch}(t))\ (\forall t \in T_m) \tag{2.3}$$

With $P_b^{dis}(t)$ and $P_b^{ch}(t)$ being respectively the discharging and charging power of the BESS at time t in kW. Equation (2.1) sets the convention that if $P_b(t)$ is positive, the BESS is discharging into the building. P_b^{max} is the maximum power of the BESS in kW and $y_{ch}(t)$ is a binary variable conditioning the authorization of charge of the BESS under specific conditions as seen in (3.1).

$$y_{ch}(t) = \begin{cases} 1 \text{ if } P_l(t) < P_c \\ 0 \text{ otherwise} \end{cases} \tag{3.1}$$

With P_c being the contract power. Constraint (3.1) is used to ensure that the BESS is never allowed to charge when the building power demand is above the contract power. It ensures that the BESS charging process does not create a power peak. The constraint has been linearized and replaced by constraints (3.2) to (3.5).

$$\frac{P_c - P_l(t)}{P_l^{max}} \leq y_{ch}(t) \ (\forall t \in T_m, y_{ch} \in \{0;1\}\ ) \tag{3.2}$$

$$y_{ch}(t)\langle 1 - \frac{P_l(t) - P_c}{P_l^{max}} \ (\forall t \in T_m, y_{ch} \in \{0;1\}) \tag{3.3}$$

With P_l^{max} the maximum attainable power of the building load demand in kW, subject to (3.4) and (3.5).

$$P_l^{max} > P_c + P_b^{max} \tag{3.4}$$

$$P_l^{max} > P_l(t) - P_c \ \ (\forall t \in T_m) \tag{3.5}$$

BESS energy is subject to constraints (4.1) to (4.5).

$$E_b(t+1) = E_b(t) + \Delta E_b(t) \ (\forall t \neq (N-1) \in T_m) \tag{4.1}$$

$$\Delta E_b(t) = \Delta \mathrm{t} \cdot \left(P_b^{ch}(t) \cdot \eta_b - \frac{P_b^{dis}(t)}{\eta_b} \right) \tag{4.2}$$

$(\forall t \in T_m)$

$$0 \leq E_b(t) \leq B_{cap} \ \ (\forall t \in T_m) \tag{4.3}$$

$$B_{cap} \ = DoD \ \cdot \ B_{totcap} \tag{4.4}$$

$$E_b(t=0) = B_{cap} \tag{4.5}$$

With B_{totcap} being the total capacity of the BESS in kWh and *DoD* its maximum depth-of-discharge. Note that B_{cap} is defined to simplify the equations and avoid integrating the *DoD* in problem (1.1) and constraint (4.1). η_b is the efficiency of the BESS bidirectional inverter assumed to be the same in charging and discharging mode. Note that the self-discharge rate of the BESS is voluntarily ignored here, as in such application, the BESS is rarely idle for long periods of time. Finally (4.5) is used only while performing simulations to initialize the value of E_b. In a real-time setting, it would be given by the BESS's SOC measurement.

The monthly power peak variable $P_{p,m}$ is subject to the constraints (5.1) to (5.2).

$$P_c \leq P_{p,m} \ (\forall m \in M) \tag{5.1}$$

$$P_l(t) + P_b \ (t) \leq P_{p,m} \ (\forall t \in T_m, \forall m \in M) \tag{5.2}$$

While solving problem defined in (1.1), the solver finds $P_b^*(t)$ which are the optimal values for the BESS power at each time step that minimize the objective function. Consequently, the solver also computes the monthly power peak value that minimizes the electricity bill. The formulation of problem (1.1) and the use of constraint (5.1) and (5.2) ensure that the monthly power peak is minimized to reduce cost by bringing the value of $P_{p,m}$ *as close to the contract power as possible. If excluded, the solver only minimizes the energy part of the bill. Which, with pricing subject to time-of-use might not reduce the monthly power peak.*

2.3. Robust optimization formulation

Problem (1.1) previously formulated assumes the building load $P_l(t)$ as a variable known with certainty, as though it were predicted perfectly. Uncertainties associated with load predictions, as described in Section 2.1, are now considered by using equation (6.1) to model the building load.

$$P_l(t) \in [\widehat{P}_l(t) - \sigma(t);\ \widehat{P}_l(t) + \sigma(t)] \ (\forall t \in T_m) \tag{6.1}$$

With $\widehat{P}_l(t)$ the forecasted value of the building load power at time t and $\sigma(t)$ the possible deviation of the forecasted building load power defined by (6.2).

$$\sigma(t) = \widehat{P}_l(t) * e_{forecast} \ (\forall t \in T_m) \tag{6.2}$$

With $e_{forecast}$ the mean percentage of error of the neural networks. This value is computed during the training process of the neural networks.

To gain more control on the conservatism of the robust approach, we use a budget of uncertainty, named gamma and noted $\mathbf{\Gamma}$, as proposed in Ref. [30]. $P_l(t)$ is then defined by (6.3).

$$P_l(t) = \widehat{P}_l(t) + \beta(P_l(t), \Gamma) \ (\forall t \in T_m) \tag{6.3}$$

With $\beta(P_l(t), \Gamma)$ the deviation of the forecasted load demand as a function of Γ, as defined in (6.4).

$$\beta(P_l(t), \Gamma) = \sigma(t)^* z^*(t) \ (\forall t \in T_m) \tag{6.4}$$

With $z^*(t) \in Z^*$ the set of optimal values of the problem defined in (7.1).

$$Z^* = \underset{z(t)\in[0,1]}{\operatorname{argmax}} \sum_{t=1}^{T} \sigma(t)^* z(t) \tag{7.1}$$

Subject to constraint (7.2)

$$\sum_{t=1}^{T} z(t) \leq \Gamma \tag{7.2}$$

With $z(t)$ *being the weight attributed to the anticipated forecasting error for each time t.*

Solving the problem defined in (7.1) allows to find the optimal values $z^*(t)$ that maximize Z^* which is then used in (6.3). In other terms, solving problem (7.1) allows to find the value of $z(t)$ *that maximizes the total prediction error that will be accounted for. With an increased value of* Γ*, more errors will be accounted for to maximize the total error. Thus, while solving (7.1) the solver increases the value of the forecasted building load during time steps where an error would have the most significant impact.*

By substituting $P_l(t)$ defined as in (6.1) in all equations found in section 2.2 and by solving problem (7.1) and (1.1) at each iteration, we can find a robust value of the power setpoint the EMS will follow to control the BESS. Computation of this setpoint is done using equation (8.1) below.

$$P_{setpoint} = \max_{t\in T} \left(\widehat{P}_l(t) - P_b^*(t)\right) \tag{8.1}$$

with $P_b^*(t)$ being the computed optimal power of the BESS at time t in kW. $P_{setpoint}$ is the power setpoint in kW sent to the controller. This value is used to control the BESS power in real time by comparing it to the real-time building demand, as explained in section 2.4.

2.4. Robust model predictive control

The proposed control architecture leverages the Model Predictive Control (MPC) framework as outlined in section 1, coupled with the robust optimization model described in Section 2.3. This two-layer architecture is depicted in Fig. 1 and integrates asynchronous optimization with real-time control to manage the operation of the Battery Energy Storage System (BESS) effectively.

The first layer, executed asynchronously every 15 min, computes the optimal power setpoint $P_{setpoint}$ used by the second layer to control the BESS's charging and discharging operations. This layer performs three critical tasks to derive the optimal setpoint. First, it aggregates input data, including historical load demand from a local database, predicted and historical outdoor temperature from an external weather API, and real-time building load measurements from the building's electricity meter. These data streams are pre-processed and fed into neural networks to forecast the building's load demand for the prediction rolling horizon T spanning from the current time step to the end of the day. The second task utilizes these forecasts as inputs to solve the robust optimization problem (7.1), which integrates bounded uncertainty through a budget parameter Γ. Finally, the minimization problem (1.1) is solved, incorporating the optimization horizon and updated constraints, to compute the optimal power setpoint using equation (8.1).

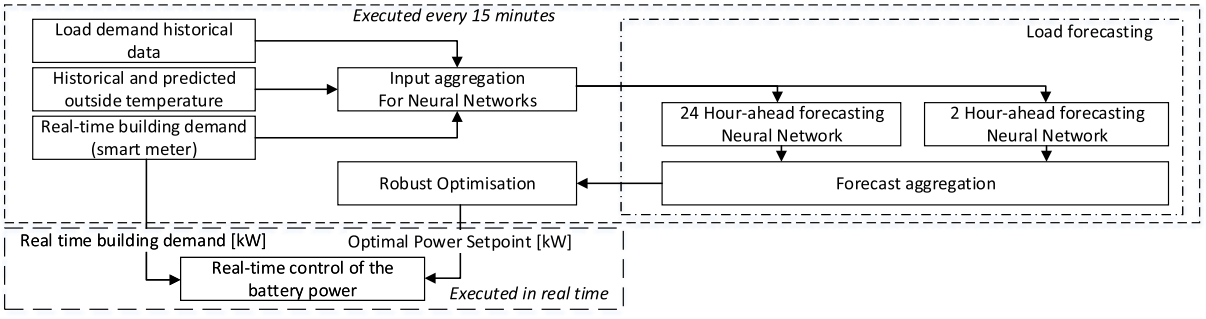

Fig. 1. Architecture of the proposed control algorithm.

The formulation of problems (7.1) and (1.1) is designed to optimize the electricity bill on a monthly scale by minimizing peak demand charges and operational costs. However, due to the inherent challenges in accurately forecasting building load over an entire month, the model adopts a daily interpretation. In this approach, prior to solving problem (1.1), the monthly power peak $P_{p,m}$ is initialized to its last known value which is updated dynamically whenever grid power exceeds the recorded peak during the current month and reset to the contracted power value at the beginning of a new month. Moreover, the rolling prediction horizon T is updated to span from the current time to the end of the day, enabling the MPC framework to adapt dynamically to daily load variations. The daily interpretation is particularly suited for the studied university campus, where nighttime energy consumption remains low due to the HVAC system's energy-saving mode and campus closure. This assumption ensures the BESS has sufficient time to recharge fully each night.

The second layer operates in real time to control the BESS using the optimal power setpoint calculated by the asynchronous layer. *Real time BESS power* $P_{b_{command}}(t)$ *is computed in the real-time layer using* equation (9.1).

$$P_{b_{command}}(t) = P_l(t) - P_{setpoint} \tag{9.1}$$

The optimal power setpoint $P_{setpoint}$ can be regarded as the maximum instantaneous power that is expected to be drawn from the grid during a day. This approach enhances robustness by decoupling the BESS control from direct dependence on load forecasting. If predictions are accurate, the comparison of $P_l(t)$ with $P_{setpoint}$ ensures the BESS power matches the optimal value computed during robust optimization. In cases of forecasting errors, the BESS adjusts dynamically to prevent grid power from exceeding $P_{setpoint}$, thereby ensuring the BESS usage maintains an optimal balance between energy use and availability. Additionally, real-time constraints are enforced to ensure the system operates within safe boundaries. These include maintaining the inverter's maximum power rating and the BESS's state of charge (SOC) within secure limits. The system also adheres to constraint (3.1), prohibiting BESS charging when the building's load exceeds the contracted power. In practice, equation (9.1) is implemented through a PID controller embedded in the bidirectional inverter, which stabilizes BESS output and prevents oscillations in response to sudden load changes.

The asynchronous nature of the first layer significantly enhances the control architecture's robustness. Tasks such as data aggregation, load forecasting, and robust optimization are time-consuming and susceptible to errors due to API failures, database connectivity issues, or unexpected disruptions. By decoupling these operations from real-time control, the system ensures continuity of the second layer even if the first layer experiences failures. The last computed $P_{setpoint}$ is retained for real-time operations, enabling uninterrupted control. Error management and redundancy mechanisms allow the asynchronous layer to recover and update the setpoint once operational, ensuring high resiliency of the overall architecture.

Finally, the integration of robust optimization within the MPC framework ensures that the optimal setpoint calculation remains resilient to forecast uncertainties. The use of a rolling horizon approach allows for continuous recalculation and adaptation to real-life events, further enhancing the system's ability to respond dynamically to changing conditions.

2.5. Use case and small-scale test bench

Our research takes place on a large university campus composed of residential, commercial, and institutional buildings as described in Ref. [15]. This case study presents a highly pertinent example for evaluating the effectiveness of the proposed control algorithm. Firstly, the unpredictability of the load is significant and imputed to the heterogeneity of building types, each characterized by its distinct load profile. Secondly, the occurrence of significant power peaks, surpassing 7 MW, renders the installation of a battery bank large enough to mitigate the entire load demand economically impractical. Moreover, the substantial power demand of the building significantly increases the power component of the electricity bill. This situation makes peak shaving especially beneficial for cost reduction. Lastly, it is postulated that successful application of the proposed algorithm in this complex scenario may facilitate its adaptability to scenarios involving smaller loads. This aspect will be explored in subsequent studies. At the time of composition, the campus did not have a BESS installed, as the present paper originated on the feasibility analysis of installing such a system. Thus, all results presented in section 3 have been created by assuming a hypothetical microgrid installed on the campus with characteristics defined in Table 1.

The billing scheme is based on 2023 Hydro-Quebec's LG tariff [31] which characteristics are presented in Table 2.

Table 1
Microgrid characteristics (represented system).

Parameter	Value
BESS total capacity B_{totcap}	2750 kWh
BESS maximum depth-of-discharge *DoD*	80 %
BESS effective capacity B_{cap}	2200 kWh
Inverter-charger maximum power P_b^{max}	500 kW
Inverter-charger CEC efficiency η_b	94.1 %

All the results presented in section 3 of the article have been created by assuming a hypothetical microgrid installed on the campus with characteristics defined in Table 1. BESS means Battery Energy Storage System. CEC efficiency refers to the efficiency rating established by the California Energy Commission (CEC) for solar inverters and other power conversion devices.

The contract power is the minimum power demand that is billed at the end of the month. It corresponds to the lowest power demand at which the algorithm must reduce the monthly peak demand to minimize power costs. This value depends on the previous month's maximum demand. However, since 5 MW is the lowest contract power eligible for this tariff, this minimum limit is used to ensure maximum effort of the control algorithm throughout the years.

Table 3 shows parameters values used to configure the control algorithm to achieve results shown in section 3.

Two typical winter and summer days, January 15, 2022, and July 10, 2023, respectively, have been selected to show the performances of the proposed algorithm. Those days represent the periods of the year with the highest power peaks due to high demand in terms of heating and cooling for the buildings.

Since the campus energy demand is progressively increasing, we chose one day in 2022 and one in 2023 to show the robustness of the algorithm throughout time. It is important to note that the neural networks used to forecast January 15th were trained with data from 2018 to end of 2021 whereas neural networks used to forecast July 10, 2023, have been updated to include training data from 2018 to end of 2022. Indeed, both neural networks are constantly learning with new historical data to adapt to the evolving load demand pattern of the building.

To achieve real time validation of the proposed control algorithm, a small-scale test bench has been created and implemented in a laboratory. Its design aims at replicating, in real time, the campus's load on a smaller scale and controlling a BESS to perform peak shaving. Its composition can be found in Table 4.

The power ratio is used to convert real time load demand to the test bench load demand. The time ratio enables faster simulations when experimenting with historical data. With selected settings, a past 24-h day can be run in 16 h. It can be further increased provided that the BESS power setpoint is scaled accordingly.

3. Results and discussion

Results are presented in Tables 5 and 6 which show the different algorithms efficiency for January 15, 2022, and July 10, 2023, respectively. The graphs show the behavior of the selected control algorithm and the final value of the daily peak power.

The first graphs of each table (Figs. 2 and 6) show the theoretical optimal power shaving for both typical days. They have been computed using historical data to prove that, given perfect predictions, the non-robust optimization model defined in section 2.2 is able to perfectly shave the load building. It also provides the optimal reference value for the setpoint used to benchmark all the presented algorithms. Both figures show that the BESS is fully discharged by the end of the day and that the load is fully shaved to the optimal setpoint computed at the beginning of the day. Decreasing further this setpoint would have necessitated more energy or power available in the BESS.

Second graphs of each table (Figs. 3 and 7) show the same typical days, but this time optimized using imperfect neural networks forecasting. The optimization model used is the linear one described in section 2.2. Without the use of the MPC framework, the computation of the setpoint is performed only once a day as soon as the building load exceeds the contract power of 5 MW. Which, for both days, corresponds to the time the heating, ventilation and cooling systems begin operating under normal conditions after night energy-saving mode. On January 15th (Fig. 3), we observe that the predicted power is close to the actual building load except early in the day from 8a.m. to 11a.m. Consequently, the computed power setpoint is significantly lower than the theoretical optimal power setpoint. Therefore, the BESS energy is rapidly emptied, resulting in the afternoon peak demand being unshaved. On July 10th (Fig. 7), the load forecasts are strictly lower than the real building demand. Which causes the computed setpoint to be lower than the optimal one. Therefore, the BESS is once again emptied early in the day, leaving the entire afternoon power demand unshaved. Those two graphs demonstrate the need for accurate forecasting and the necessity of a correction process, such as the proposed MPC approach. One objective of present work is to demonstrate that the proposed algorithm can improve those results.

Using the non-robust MPC algorithm described in section 2.4, we can observe on the third graphs of each table (Figs. 4 and 8), that the power setpoint is continuously evolving throughout the day, being recalculated every 15 min. For January 15th (Fig. 4), we observe that the system is starting its load shaving effort in the morning, with a setpoint value greatly below the optimal. Looking at the BESS power, we observe that the maximum power of the inverter is attained around 8a.m. due to a low setpoint and a high unforeseen demand causing the inability of the control system to shave the grid power at the computed setpoint value. In response, the MPC algorithm rapidly adapts and starts increasing the setpoint value. Doing so, the BESS can shave almost entirely the grid power at the final setpoint value. However, due to the large setpoint error at the beginning of the day, the BESS is emptied before the last high demand period, leaving a power peak 3.16 % above the optimal but 1.38 % lower than the one reached without the MPC algorithm

Table 2
Billing characteristics.

Parameter	Value
Price of power demand C_p	14.667 $/kW
Price of energy C_e	3.83 ¢/kWh
Contract power of the campus P_c	5000 kW

The billing scheme used in the article is based on 2023 Hydro-Quebec's LG tariff [31] which characteristics are presented in Table 2. The contract power is the minimum power at which the building will be billed for power at the end of the month.

Table 3
Algorithm parameters.

Parameter	Value
Mean percentage of errors of ANN forecasting used for robust optimization $e_{forecast}$	3 %
Location (for weather API)	Montréal, QC, CA
State of charge fee of BESS λ_{ch}	0.2 ¢/kWh
Maximum theoretical power demand of the load P_l^{max}	12 000 kW
Initial Power Setpoint $P_{setpoint}(0)$	5000 kW
Timestep Duration Δt	0.25 h

Table III shows parameters values used to configure the control algorithm to achieve results shown in section 3. ANN means Artificial Neural Networks which are used to forecast the load demand. BESS means Battery Energy Storage System.

Table 4
Test bench equipment.

Parameter	Total capacity/power
6 Programmable loads [32]	27 kW
4 Lithium Ferro Phosphate (LFP) batteries [33]	15.2 kWh
1 controllable inverter-charger [34]	6.8 kW
Power ratio	500
Time ratio	1.5

To achieve real time validation of the proposed control algorithm, a small-scale test bench has been created. Its design aims at replicating, in real time, the campus's load on a smaller scale and controlling a battery energy storage system (BESS) to perform peak shaving. Its composition can be found in Table 4. The power ratio is used to convert real time load demand to the test bench load demand. The time ratio enables faster simulations when experimenting with historical data. With selected settings, a past 24-h day can be run in 16 h. It can be further increased provided that the BESS power setpoint is scaled accordingly.

shown in Fig. 3. Thus, proving the superiority of the MPC algorithm.

Looking at graphs for July 10th (Fig. 8), we can observe, contrary to what was seen without the MPC (Fig. 7), the computed setpoint continuously evolving during the morning, even after the start of the shaving effort. Doing so, the control algorithm prevents the discharge of the BESS when unnecessary. Then, it stabilizes for the entirety of the day. The final daily power peak is equal to the final value of the setpoint which is 2.38 % above the theoretical optimal and 2.43 % below the daily peak reached without the MPC algorithm as shown in Fig. 7 thanks to the BESS not being emptied during the day. However, one could observe that the BESS energy at the end of the day is far from being empty, showing that this algorithm could further be improved.

The last graph of each table (Figs. 5 and 9) shows the same days optimized with the final proposed algorithm, that is the robust MPC implementation. Thanks to robust optimization, we can observe that some of the load forecasts' values are increased under the assumption that the forecast demand is lower than the real demand. The rectified forecasts are scattered across the entire peak period and are more frequent with higher values of the budget of uncertainty named gamma as described in section 2.3.

For January 15th, we observed earlier on Fig. 4 that, when using the non-robust MPC algorithm, the BESS was emptied earlier than the occurrence of the final peak. Whereas, on Fig. 5, using robust optimization with a gamma value of 5, the setpoint value is higher, enabling less energy loss in the BESS at the beginning of the day and a more conservative adaptation of its value throughout the day. This results in the final peak period of the day to be fully shaved, thanks to the remaining energy in the BESS at the time of its occurrence. Thus, the robust-MPC algorithm lowers the final daily peak to a level which is 2.19 % better than the final peak obtained using the MPC algorithm without robustness and only 0.99 % (61 kW) above the theoretical optimal.

For July 10th, on Fig. 8, we observed earlier that the MPC algorithm was performing better than the standard optimization but was still higher than the theoretical optimal. On Fig. 9, we can observe that via addition of robust optimization into the MPC algorithm, the final peak power reached at the end of the day is only 0.07 % (3.5 kW) above the optimal. Comparing both figures, we can observe that the setpoint follows the same pattern whether robust optimization is used or not. However, thanks to robust optimization, the value of the setpoint at the beginning of the peak period is more appropriate than its counterpart without robust optimization. In fact, by evaluating the worst-case scenario, the robust MPC was able to understand that the load demand would not go as high as the non-robust MPC estimated, thus reducing the value of the setpoint.

For both days, the Robust-MPC algorithm performs better than its non-robust counterpart.

3.1. Algorithms comparison and gamma value optimization

Figs. 10 and 11 below show the final daily power peak for each presented algorithm. That is, the theoretical optimal using perfect predictions, noted *Optimal*, the non-MPC with standard optimization, noted *SO*, the non-MPC with robust optimization with different values of gamma, noted *ROx*, x being the value of gamma, the MPC with standard optimization noted *MPC SO* and the Robust MPC

Table 5
Comparison of algorithms for January 15, 2022.

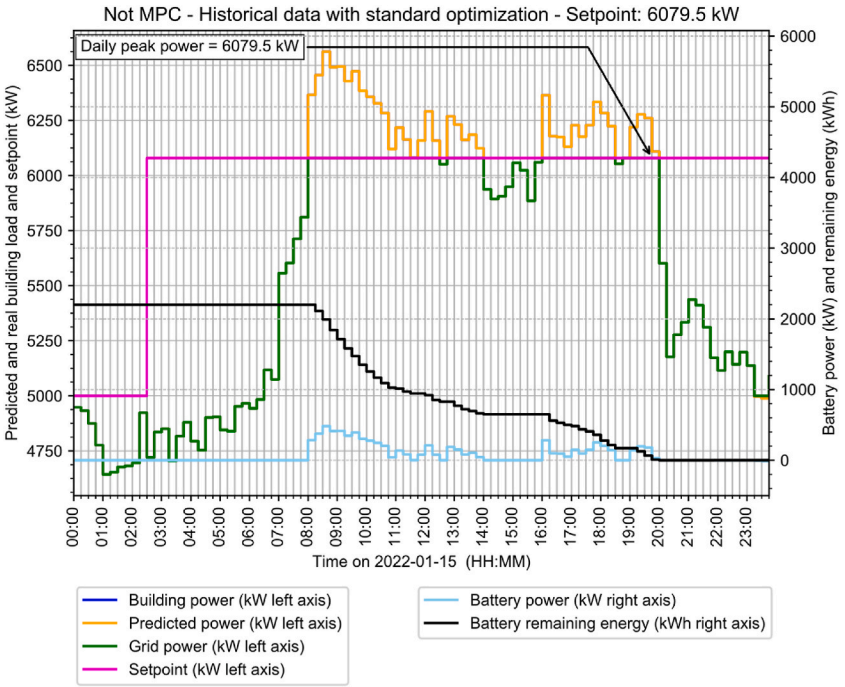

The theoretical optimal peak shaving. It serves as reference to benchmark all other algorithms.
Algorithm used:
- Non-MPC
- Historical data (i.e., perfect predictions)
- Non-robust optimization

Performances:
- Setpoint is computed at the beginning of the day
- The setpoint is fixed at 6079.5 kW
- The final daily peak is equal to the setpoint.
- Final state of the BESS: emptied when building's load reduces below the setpoint (19h45).

Figure 2 - 2022-01-15 - Theoretical perfect peak shaving

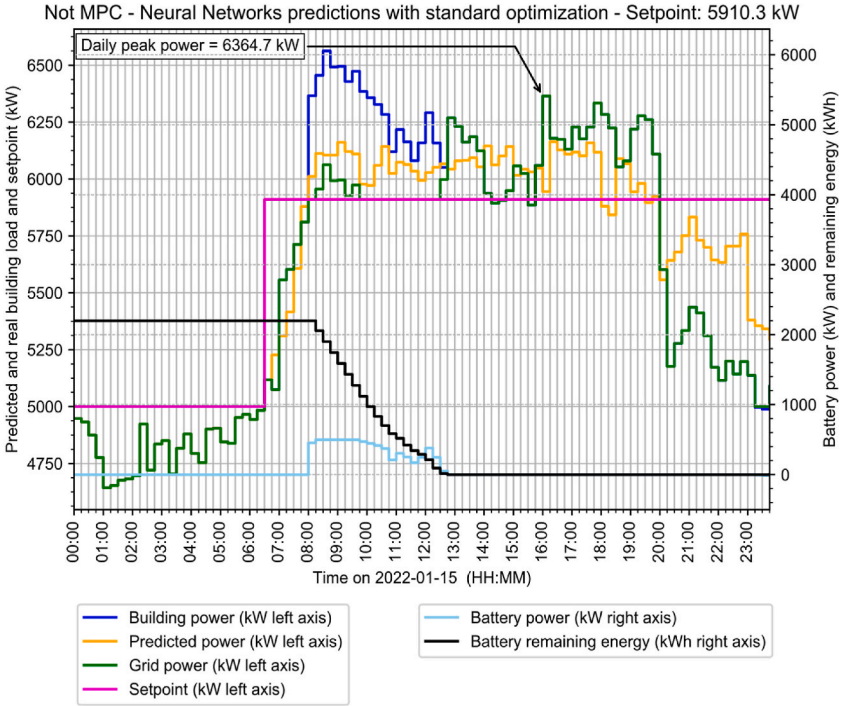

Non-MPC Standard optimization with neural networks forecasting. This case demonstrates the relative accuracy of the neural networks forecasting. The large error occurring at the beginning of the day combined with the absence of MPC explains poor results for this algorithm.
Algorithm used:
- Non-MPC
- **Neural Networks predictions**
- Non-robust optimization

Performances:
- Setpoint is computed once, when the load exceeds 5 MW.
- The setpoint is fixed at 5910.3 kW.
- The final daily peak is 4.48 % (285.2 kW) higher than the optimal.
- Final state of the BESS: emptied early in the day. (12h30 i.e., 7h15 earlier than optimal)

Figure 3 – 2022-01-15 – Non-MPC standard optimization with neural networks

(*continued on next page*)

Table 5 (*continued*)

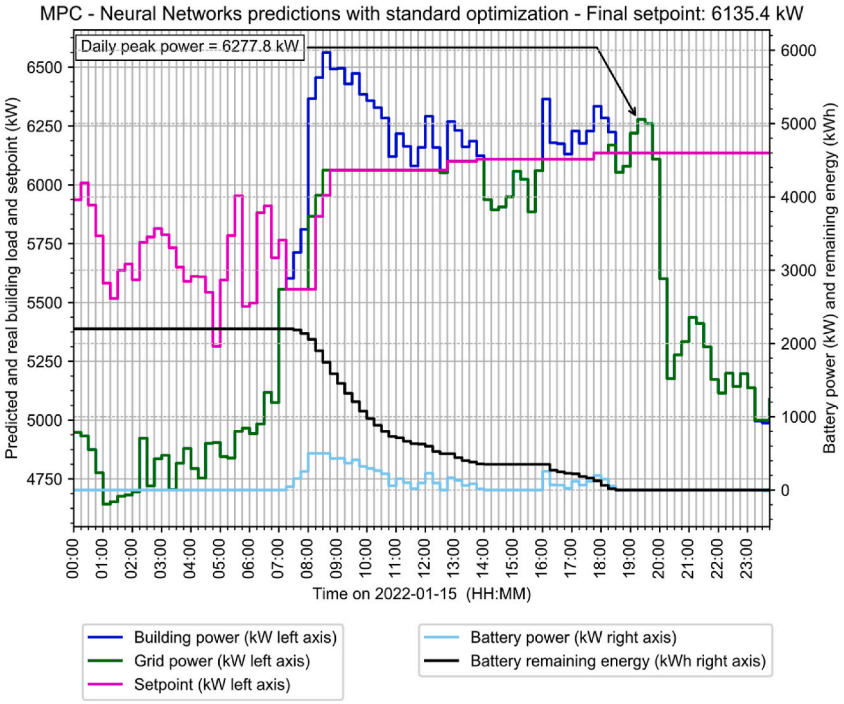

MPC Standard optimization with neural networks forecasting. This case demonstrates the efficiency of the MPC approach. The large forecast error occurring previously is corrected throughout the day. However, they still over-discharge the BESS. Reducing peak shaving impact.
Algorithm used:
-MPC
-Neural Networks predictions
-Non-robust optimization
Performances:
- Setpoint is computed each 15 min.
- The final setpoint is fixed at 6135.4 kW.
- The final daily peak is 3.16 % (198.3 kW) higher than the optimal.
- The final daily peak is 1.38 % (86.9 kW) lower than the previous results (Fig. 3).

Final state of the BESS: emptied early in the day. (18h30 i.e., 1h15 earlier than optimal)

Figure 4 – 2022-01-15 – MPC standard optimization with neural networks.

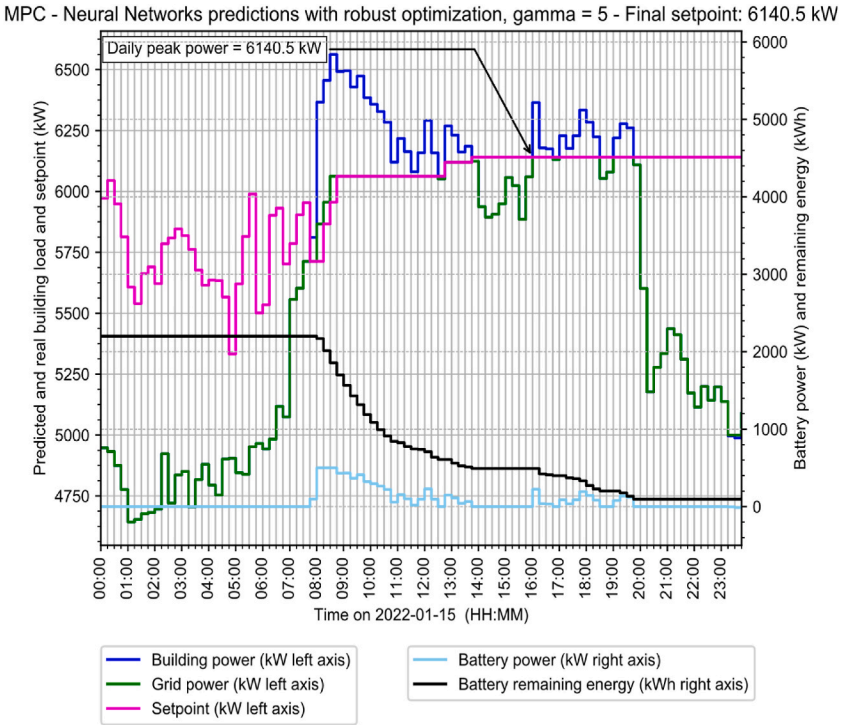

Robust MPC with neural networks forecasting. This case demonstrates the superiority of the proposed Robust-MPC algorithm.
Algorithm used:
- MPC
- Neural Networks predictions
- **Robust** optimization (Gamma = 5)

Performances:
- Setpoint is computed each 15 min.
- The final setpoint is fixed at 6140.5 kW.
- The final daily peak is 0.99 % (60.9 kW) higher than the optimal.
- The final daily peak is 2.19 % (137.3 kW) lower than the previous results (Fig. 4).

Final state of the BESS: 4.6 % remaining energy when the building load drops below the setpoint. (19h45 i.e., same time as optimal.)

Figure 5 – 2022-01-15 – Robust MPC optimization with neural networks

optimization with different values of gamma, noted *MPC ROx*. On both figures, gamma ranges from 5 to 25.

Results show the impact of gamma on the value of the peak power reached at the end of the day. It can be observed that the use of robust optimization without the MPC approach (*SO* and *ROx*) necessitates a large value of gamma, at 20 or 25, to start decreasing the final daily power peak. Which indicates important forecasting errors. Indeed, a long peak period ranging from 8a.m. to 8p.m.

Table 6
Comparison of algorithms for July 10, 2023.

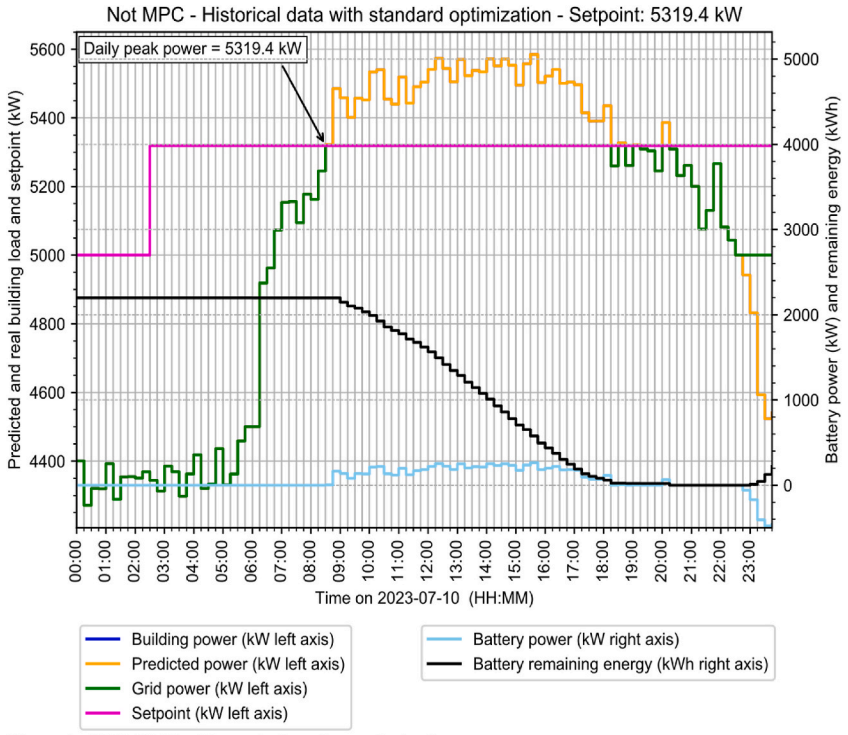

The theoretical optimal peak shaving. It serves as reference to benchmark all other algorithms.
Algorithm used:
- Non-MPC
- Historical data (i.e., perfect predictions)
- Non-robust optimization

Performances:
- Setpoint is computed at the beginning of the day.
- The setpoint is fixed at 5319.4 kW.
- The final daily peak is equal to the setpoint.

Final state of the BESS: emptied when building's load reduces below the setpoint (20h15).

Figure 6 - 2023-07-10 - Theoretical perfect peak shaving

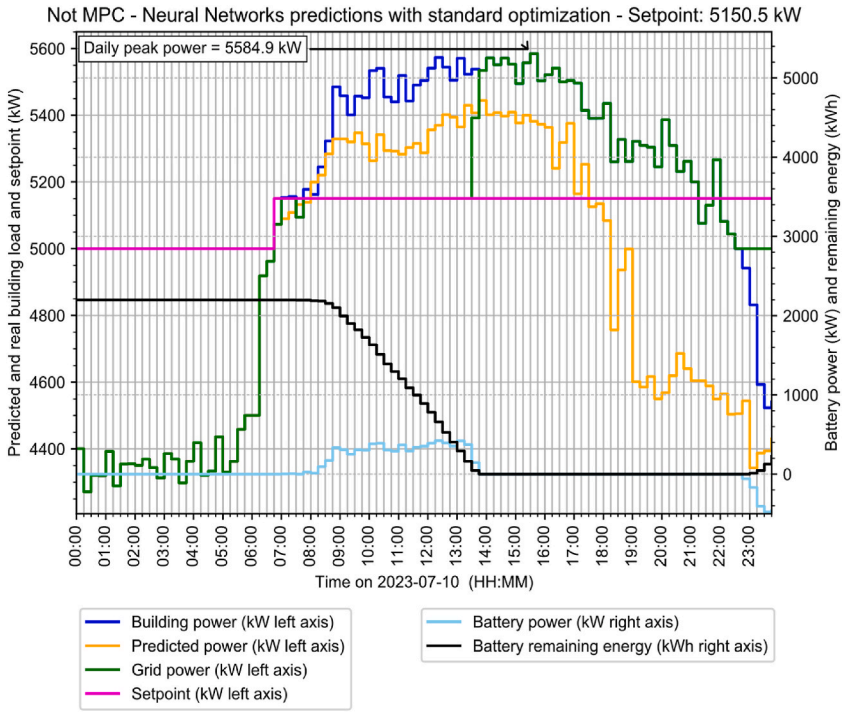

Non-MPC Standard optimization with neural networks forecasting. This case demonstrates the relative accuracy of the neural networks forecasting. The large error occurring throughout the day combined with the absence of MPC explains poor results for this algorithm.
Algorithm used:
- Non-MPC
- **Neural Networks predictions**
- Non-robust optimization

Performances:
- Setpoint is computed once, when the load exceeds 5 MW.
- The setpoint is fixed at 5150.5 kW.
- The final daily peak is 4.75 % (265.5 kW) higher than the optimal.

Final state of the BESS: emptied early in the day. (12h30 i.e., 7h45 earlier than optimal)

Figure 7 – 2023-07-10 – Non-MPC standard optimization with neural networks

(*continued on next page*)

Table 6 (*continued*)

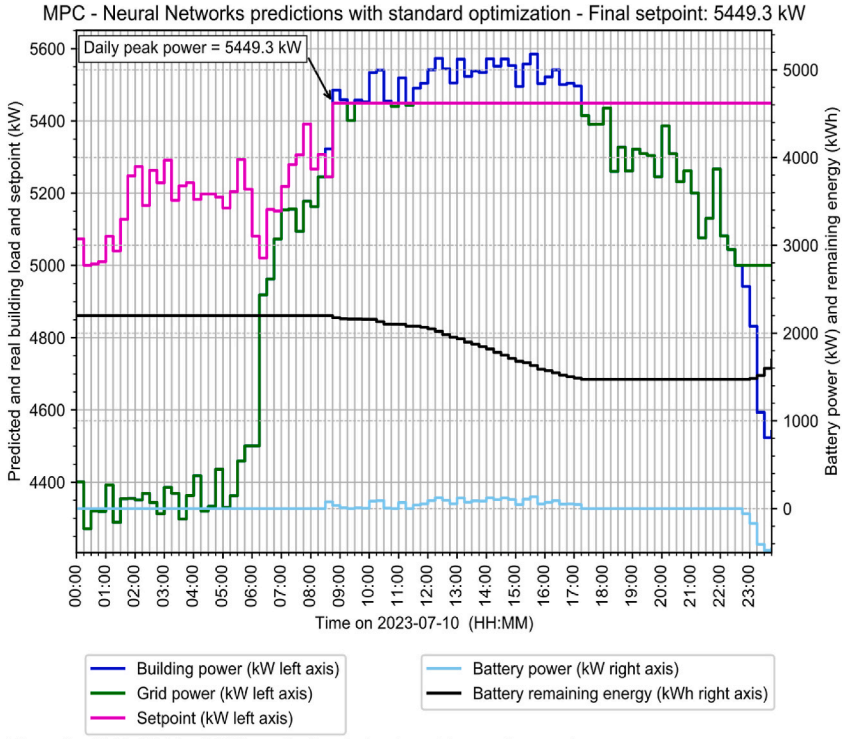

MPC Standard optimization with neural networks forecasting. This case demonstrates the efficiency of the MPC approach. The large forecast error occurring previously is corrected throughout the day. However, over-estimations of highest load consumption drastically reduce the peak shaving effort.
Algorithm used:
- **MPC**
- Neural Networks predictions
- Non-robust optimization

Performances:
- Setpoint is computed each 15 min.
- The final setpoint is fixed at 5449.3 kW.
- The final daily peak is 2.38 % (129.9 kW) higher than the optimal.
- The final daily peak is 2.43 % (135.7 kW) lower than the previous results (Fig. 7).

Final state of the BESS: 67 % remaining energy when the building load drops below the setpoint. (19h45 i.e., same time as optimal.)

Figure 8 – 2023-07-10 – MPC standard optimization with neural networks

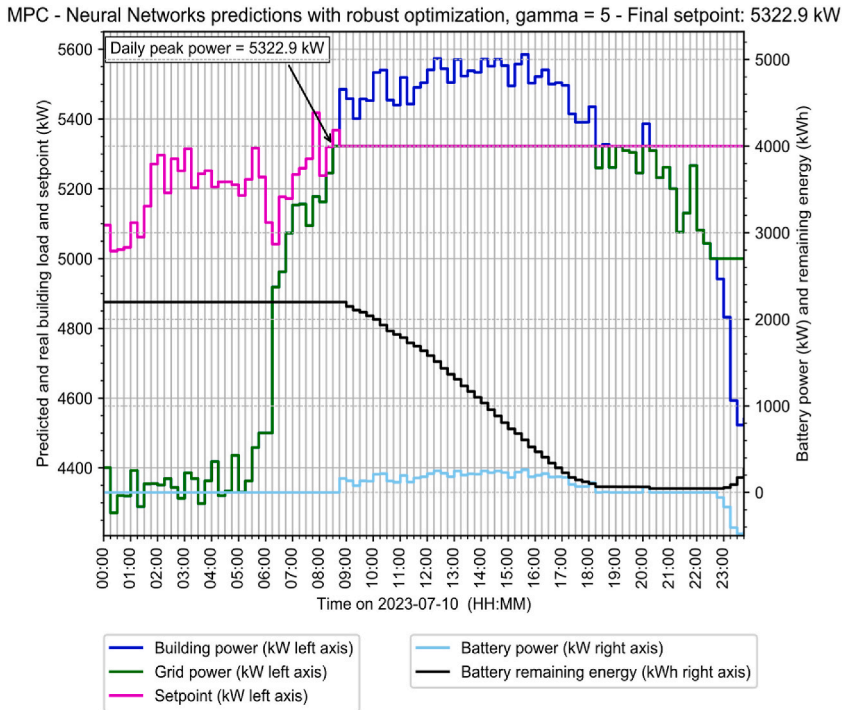

Robust MPC with neural networks forecasting. This case demonstrates the superiority of the proposed Robust-MPC algorithm.
Algorithm used:
- MPC
- Neural Networks predictions
- **Robust** optimization (Gamma = 5)

Performances:
- Setpoint is computed each 15 min.
- The final setpoint is fixed at 5322.9.5 kW.
- The final daily peak is 0.06 % (3.5 kW) higher than the optimal.
- The final daily peak is 2.32 % (126.4 kW) lower than the previous results (Fig. 8).

Final state of the BESS: 2.25 % remaining energy when the building load drops below the optimal setpoint. (20h15 i.e., same time as optimal.)

Figure 9 – 2023-07-10 – Robust MPC optimization with neural networks

corresponds to forty-eight-quarter hours. Using a gamma value of 25 means that we apply the potential forecasting error on 52 % of the peak period. The low accuracy of forecasting is explained by the fact that once the prediction has been made at the beginning of the day, its accuracy quickly deteriorates as the further time advances in the day. We concluded that the non-MPC algorithm required

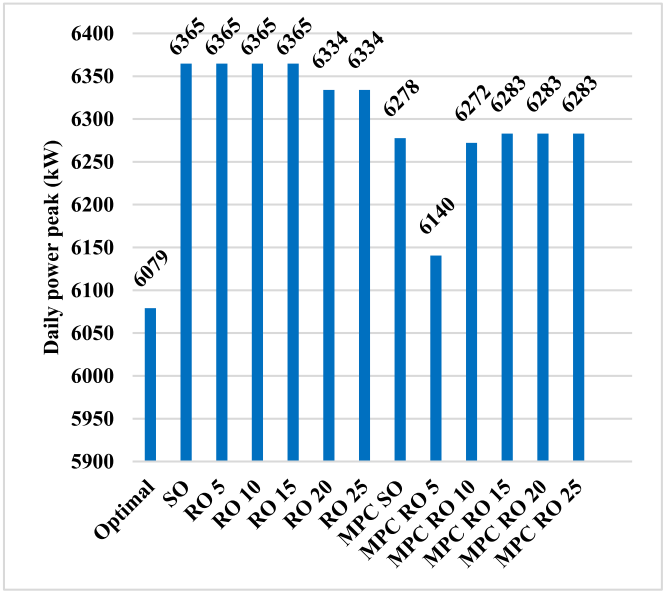

Figs. 10. 2022-01-15 - Maximum peak power reached using different algorithms.

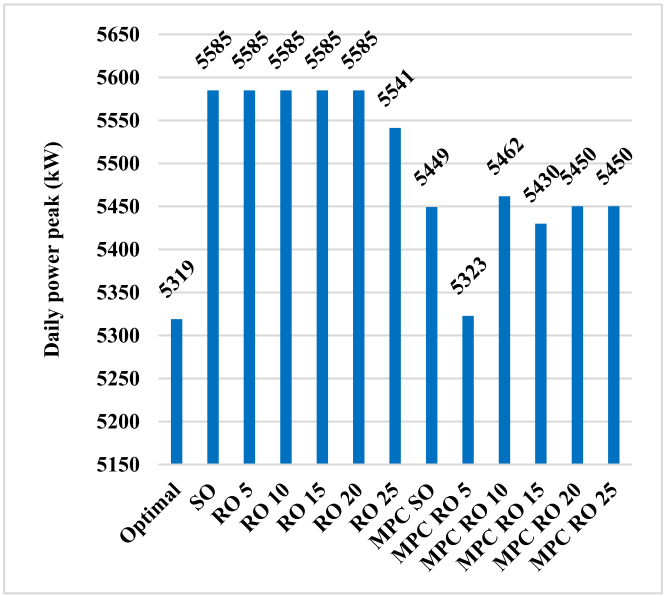

Figs. 11. 2023-07-10 - Maximum peak power reached using different algorithms.

improvements that the use of robust optimization alone was not able to provide. Therefore, demonstrating the necessity of the MPC approach.

On the other hand, when using the MPC approach, we can observe on both Figs. 10 and 11 that robust MPC (*MPC ROx*) is able to significantly improve the result of its non-robust counterpart (*MPC SO*), and that it does so with a small value of gamma. We observe that once the optimal value of gamma has been reached, increasing its value only increases the daily power peak as robust optimization is conservative in essence. Nevertheless, an inflection point can be observed, demonstrating that an optimal value of gamma can be found.

For July 10th, we can observe on Fig. 11 that the daily peak power is 5450 kW with a gamma value of zero (*MPC SO*), representing the MPC algorithm without robust optimization. The daily peak power reaches a minimum value for a gamma value of 5 (*MPC RO5*). From this value, increasing further its value deteriorates results as it increases the final daily peak power. The same behavior can be observed for January 15th (Fig. 10). Despite the deterioration in results observed with an increase in gamma beyond the inflection

point, the outcome almost consistently remains close to the performance level of the algorithm that does not incorporate robust optimization.

Finally, it is worth highlighting that both typical days exhibit the same optimal gamma value. Through an in-depth analysis conducted over 730 days (two years), we determined that a gamma value of 5 is optimal for our specific use case, as it was the most frequently identified as the best-performing value. In fact, Fig. 12 illustrates the total savings achieved on monthly bills using all proposed algorithms over the same two-year period, spanning from January 2023 to December 2024. The results demonstrate that the robust MPC algorithm with a gamma value of 5 outperforms its counterpart, delivering savings exceeding 56 000 CAD over the two-year period.

3.2. Real time implementation and validation

Fig. 13 presents the results obtained on the small-scale test bench, as described in Section 2.5, corresponding to the simulated outcomes depicted on Fig. 9. The presence of some noise is attributed to the inherent measurement inaccuracies of the test bench. Additionally, the BESS achieves a SOC of 22 % at the end of the day. This outcome is intentional, as the test bench measures the total BESS capacity rather than the effective capacity that can be seen on the simulation results and that it maintains the state of charge above 20 % to mitigate battery degradation.

These findings demonstrate that, in real-time applications, the algorithm effectively replicates the simulation results with high accuracy.

4. Conclusion

This research investigated the efficiency of a robust optimization model integrated within a model predictive control (MPC) framework, leveraging neural network-based forecasting to perform peak shaving in a large university campus. The study demonstrated that the MPC approach, due to its dynamic re-evaluation of the optimal power setpoint, consistently outperformed traditional non-MPC methods in managing energy consumption and reducing peak demand charges. A detailed analysis of the robust optimization model revealed that, although inherently conservative, the inclusion of robustness significantly enhanced the algorithm's performance when the budget of uncertainty (gamma) was appropriately tuned. This finding underscores the dual benefits of robustness: ensuring reliability under uncertainty and optimizing performance.

The proposed algorithm was successfully validated on a small-scale test bench designed to emulate real-world microgrid conditions. This practical demonstration confirmed its applicability to real-life scenarios, highlighting its scalability and adaptability. However, the use of neural networks introduces a key limitation: the need for extensive historical data from the target building for effective training. Additionally, determining and fine-tuning the value of gamma remains an empirical process that requires ongoing adjustments to account for variations in building load profiles and demand patterns. Future research will address these limitations by developing methodologies for efficient gamma-tuning and exploring techniques to reduce the dependency on large datasets. Furthermore, the hypothesis that the proposed algorithm achieves similar results in smaller commercial buildings remains to be tested.

This study contributes significantly to the field of peak demand management by demonstrating that battery energy storage systems can be effectively controlled using a robust MPC framework with neural network-based forecasting. The novelty of this work lies in the integration of neural networks within a robust MPC framework that explicitly incorporates a budget of uncertainty. This unique combination enables accurate load forecasting while ensuring the control strategy remains resilient to prediction errors and operational uncertainties. Importantly, this research highlights the potential for intelligent energy management systems to optimize energy use and reduce operational costs in diverse building types, including institutional, commercial, and residential complexes. By integrating robust forecasting and adaptive control techniques, this study offers a practical and innovative solution for energy-efficient building design and operation, addressing the growing need for sustainable and resilient building energy systems.

CRediT authorship contribution statement

Nicolas Mary: Writing – original draft, Visualization, Validation, Software, Resources, Methodology, Investigation, Formal analysis, Data curation, Conceptualization. **Louis-A. Dessaint:** Writing – review & editing, Validation, Supervision, Resources, Project administration, Funding acquisition.

Data availability

Research data includes confidential data thus were not made publicly available.

Declaration of generative AI and AI-assisted technologies in the writing process

During the preparation of this work, the authors used ChatGPT [35] solely to improve the readability and language of the manuscript. After using this tool, the authors reviewed and edited the content as needed and take full responsibility for the content of the published article.

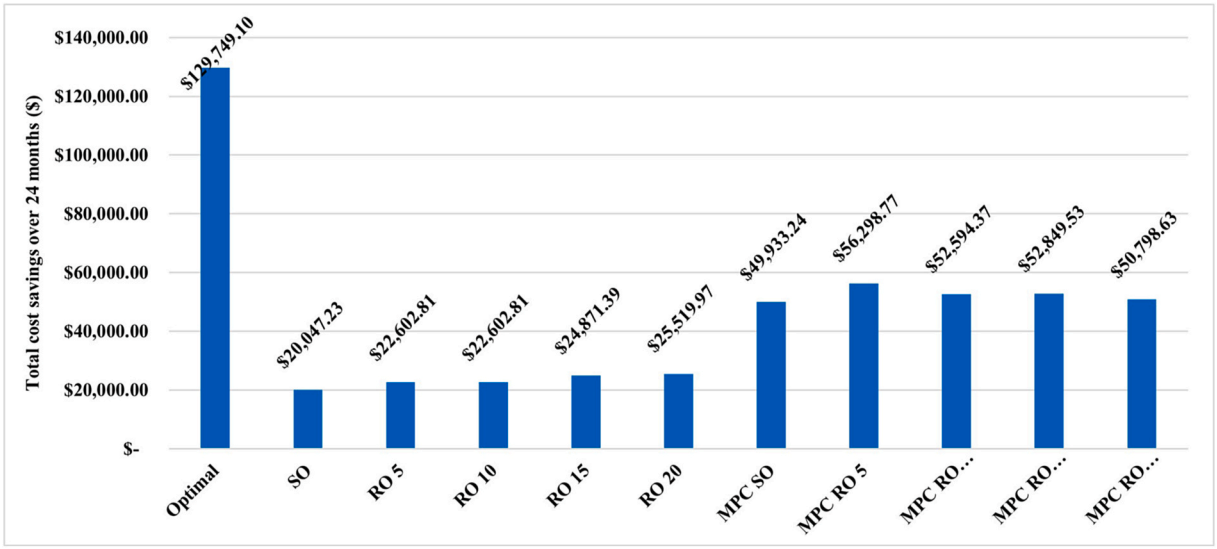

Fig. 12. Total bill savings from January 2022 to December 2023 using different algorithms.

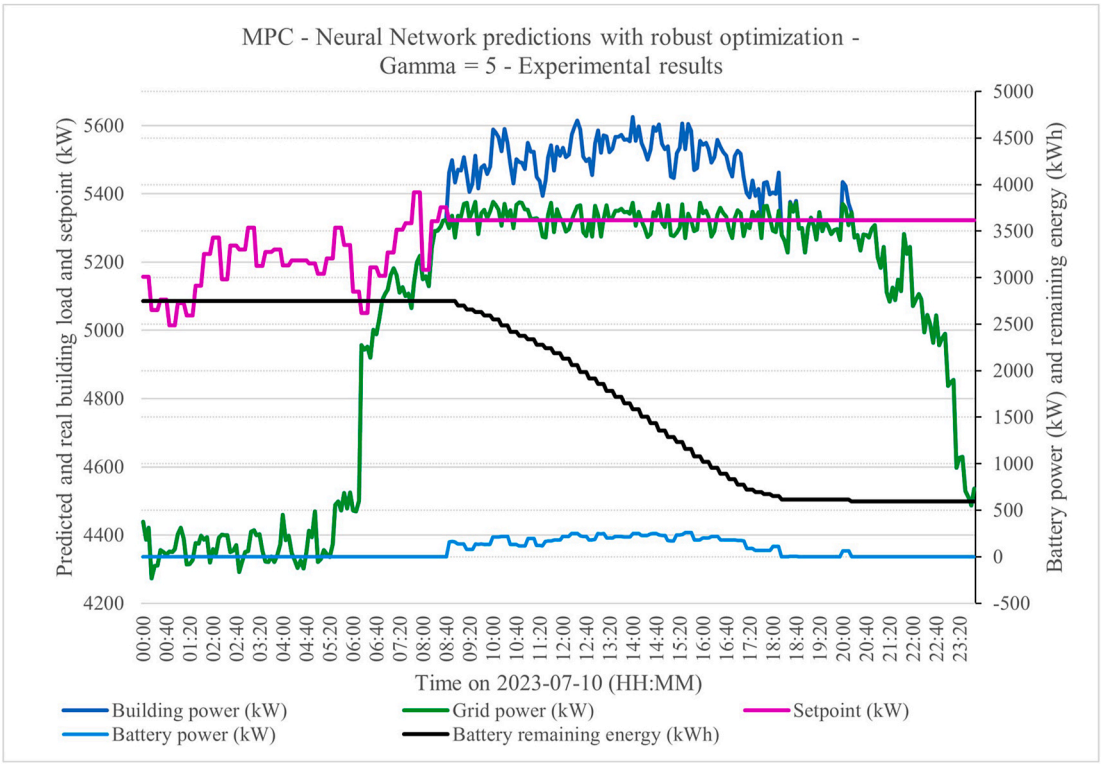

Fig. 13. – Experimental results on test bench - 2023-07-10 - MPC with robust optimization using a gamma value of 5 and neural networks predictions.

Declaration of competing interest

The authors declare that they have no known competing financial interests or personal relationships that could have appeared to influence the work reported in this paper.

Acknowledgement & Funding sources

The research work was supported by École de Technologie Supérieure (ÉTS), vadimUS conseils inc. (vadiMAP - www.vadimap.com), dcbel inc., innovÉÉ and Natural Sciences and Engineering Research Council of Canada (NSERC) under a joint research and development grant. The authors would gratefully acknowledge the facilities provided by ÉTS, particularly for the creation of the test bench that made validation of this article possible.

References

[1] Annual Energy outlook - U.S. Energy Information Administration (EIA)'. Accessed: March. 29, 2024. [Online]. Available: https://www.eia.gov/outlooks/aeo/narrative/index.php.
[2] 'Énergir - dual energy for business', Energir [Online]. Available: https://energir.com/en/business. (Accessed 20 October 2024).
[3] D.A. Zaki, M. Hamdy, A review of electricity tariffs and enabling solutions for optimal energy management, Energies 15 (22) (Jan. 2022) 22, https://doi.org/10.3390/en15228527.
[4] M. Uddin, M.F. Romlie, M.F. Abdullah, S. Abd Halim, A.H. Abu Bakar, T. Chia Kwang, A review on peak load shaving strategies, Renew. Sustain. Energy Rev. 82 (P3) (2018) 3323–3332.
[5] K. Bäcklund, M. Molinari, P. Lundqvist, B. Palm, Building occupants, their behavior and the resulting impact on energy use in campus buildings: a literature review with focus on smart building systems, Energies 16 (17) (Jan. 2023) 17, https://doi.org/10.3390/en16176104.
[6] H.T. Ebuy, H. Bril El Haouzi, R. Benelmir, R. Pannequin, Occupant behavior impact on building sustainability performance: a literature review, Sustainability 15 (3) (Jan. 2023) 3, https://doi.org/10.3390/su15032440.
[7] Y. Ozawa et al., 'Data-driven HVAC Control Using Symbolic Regression: Design and Implementation', Apr. 06, 2023, *arXiv*: arXiv:2304.03078. Accessed: October. 20, 2024. [Online]. Available: http://arxiv.org/abs/2304.03078.
[8] W. Cole, A. Karmakar, Cost projections for utility-scale battery storage: 2023 update, Renew. Energy (2023).
[9] V. Saxena, N. Kumar, U. Nangia, Computation and optimization of BESS in the modeling of renewable energy based framework, Arch Computat Methods Eng 31 (4) (May 2024) 2385–2416, https://doi.org/10.1007/s11831-023-10046-7.
[10] B.-R. Ke, T.-T. Ku, Y.-L. Ke, C.-Y. Chuang, H.-Z. Chen, Sizing the battery energy storage system on a university campus with prediction of load and photovoltaic generation, IEEE Trans. Ind. Appl. 52 (2) (Mar. 2016) 1136–1147, https://doi.org/10.1109/TIA.2015.2483583.
[11] M.E. Raoufat, B. Asghari, R. Sharma, Model predictive BESS control for demand charge management and PV-utilization improvement, in: 2018 IEEE Power Energy Society Innovative Smart Grid Technologies Conference (ISGT), Feb. 2018, pp. 1–5, https://doi.org/10.1109/ISGT.2018.8403403.
[12] A. Parisio, E. Rikos, L. Glielmo, A model predictive control approach to microgrid operation optimization, IEEE Trans. Control Syst. Technol. 22 (5) (Sep. 2014) 5, https://doi.org/10.1109/TCST.2013.2295737.
[13] P.-A. Jaboulay, W. Zhu, X. Niu, X. Pan, S. Gao, Real-time energy management optimization using model predictive control on a microgrid demonstrator, in: 2017 IEEE International Conference on Energy Internet (ICEI), Apr. 2017, pp. 226–231, https://doi.org/10.1109/ICEI.2017.47.
[14] I. Novickij, G. Joós, Model predictive control based approach for microgrid energy management, in: 2019 IEEE Canadian Conference of Electrical and Computer Engineering (CCECE), May 2019, pp. 1–4, https://doi.org/10.1109/CCECE.2019.8861781.
[15] H. Dagdougui, F. Bagheri, H. Le, L. Dessaint, Neural network model for short-term and very-short-term load forecasting in district buildings, Energy Build. 203 (Nov. 2019) 109408, https://doi.org/10.1016/j.enbuild.2019.109408.
[16] X. Li, X. Cao, C. Li, B. Yang, M. Cong, D. Chen, A coordinated peak shaving strategy using neural network for discretely adjustable energy-intensive load and battery energy storage, IEEE Access 8 (2020) 5331–5338, https://doi.org/10.1109/ACCESS.2019.2962814.
[17] S. Chapaloglou, et al., Smart energy management algorithm for load smoothing and peak shaving based on load forecasting of an island's power system, Appl. Energy 238 (Mar. 2019) 627–642, https://doi.org/10.1016/j.apenergy.2019.01.102.
[18] G. Van Kriekinge, C. De Cauwer, N. Sapountzoglou, T. Coosemans, M. Messagie, Peak shaving and cost minimization using model predictive control for uni- and bi-directional charging of electric vehicles, Energy Rep. 7 (Nov. 2021) 8760–8771, https://doi.org/10.1016/j.egyr.2021.11.207.
[19] A. Chaouachi, R.M. Kamel, R. Andoulsi, K. Nagasaka, Multiobjective intelligent energy management for a microgrid, IEEE Trans. Ind. Electron. 60 (4) (Apr. 2013) 4, https://doi.org/10.1109/TIE.2012.2188873.
[20] P. Li, et al., Multi-objective robust optimization of microgrid system with electric vehicles and new renewable energy, in: 2020 5th International Conference on Power and Renewable Energy (ICPRE), Sep. 2020, pp. 351–355, https://doi.org/10.1109/ICPRE51194.2020.9233187.
[21] G.A.H. Pawitan, J.-S. Kim, MPC-based power management of renewable generation using multi-ESS guaranteeing SoC constraints and balancing, IEEE Access 8 (2020) 12897–12906, https://doi.org/10.1109/ACCESS.2019.2962807.
[22] S. Rahim, Z. Wang, P. Ju, Overview and applications of Robust optimization in the avant-garde energy grid infrastructure: a systematic review, Appl. Energy 319 (Aug. 2022) 119140, https://doi.org/10.1016/j.apenergy.2022.119140.
[23] S. Rahim, P. Siano, A survey and comparison of leading-edge uncertainty handling methods for power grid modernization, Expert Syst. Appl. 204 (Oct. 2022) 117590, https://doi.org/10.1016/j.eswa.2022.117590.
[24] J. Yang, C. Su, Robust optimization of microgrid based on renewable distributed power generation and load demand uncertainty, Energy 223 (May 2021) 120043, https://doi.org/10.1016/j.energy.2021.120043.
[25] E. Roos, D. Den Hertog, Reducing conservatism in robust optimization, Inf. J. Comput. (May 2020) 913, https://doi.org/10.1287/ijoc.2019.0913, ijoc.2019.
[26] J. Zhou, J. Zhang, Z. Qiu, Z. Yu, Q. Cui, X. Tong, Two-stage robust optimization for large logistics parks to participate in grid peak shaving, Symmetry 16 (8) (Aug. 2024) 8, https://doi.org/10.3390/sym16080949.
[27] Y. Zhang, T. Lan, W. Hu, A two-stage robust optimization microgrid model considering carbon trading and demand response, Sustainability 15 (19) (Jan. 2023) 19, https://doi.org/10.3390/su151914592.
[28] D. Dongol, T. Feldmann, M. Schmidt, E. Bollin, A model predictive control based peak shaving application of battery for a household with photovoltaic system in a rural distribution grid, Sustainable Energy, Grids and Networks 16 (Dec. 2018) 1–13, https://doi.org/10.1016/j.segan.2018.05.001.
[29] Ni Mary, Y. Geli, H. Liu, L.-A. Dessaint, Neural network based predictive algorithm for peak shaving application using behind the meter battery energy storage system. Presented at the PES General Meeting 2023, 2023.
[30] D. Bertsimas, M. Sim, The price of robustness, Oper. Res. 52 (Feb. 2004) 35–53, https://doi.org/10.1287/opre.1030.0065.
[31] Rate LG – Business'. Accessed: November. 18, 2024. [Online]. Available: https://www.hydroquebec.com/business/customer-space/rates/rate-lg-general-rate-large-power-customers.html.
[32] Programmable AC Electronic Load', Chroma Systems Solutions, Inc. Accessed: August. 21, 2024. [Online]. Available: https://www.chromausa.com/product/programmable-ac-electronic-load-63800/.
[33] 'SimpliPhi - PHI 3.8-M - 48V', Frankensolar Shop. Accessed: August. 21, 2024. [Online]. Available: https://shop.frankensolar.ca/simpliphi-phi-3-8-48v/.
[34] 'XW Pro 120/240 V', Schneider Electric Solar America. Accessed: August. 21, 2024. [Online]. Available: https://solar.se.com/us/en/product/xw-pro-120-240v/.
[35] ChatGPT'. Accessed: October. 20, 2024. [Online]. Available: https://chatgpt.com.

Nomenclatures

Abbreviations

2HA: 2-hours ahead
24HA: 24-hours ahead
ANN: Artificial Neural Network
BESS: Battery Energy Storage System
CEC: CEC efficiency refers to the efficiency rating established by the California Energy Commission (CEC) for solar inverters and other power conversion devices
EMS: Energy Management System
kW: Kilowatt
kWh: Kilowatt hour
MPC: Model Predictive Control
MW: Megawatt
NN(s): Neural Network(s)
RO: Robust Optimization
ROx: Robust Optimization with gamma equal to x
SO: Standard Optimization
SOC: State of Charge of the BESS

Mathematical symbols

Δt: Time step duration in hours
t: Current time step
m: Current month
M: Natural number set with index m of size 12 corresponding to each month in a Gregorian year
T_m: A nonnegative integer set with index t of size N that will vary according to the number of days in the month m and the resolution of the used data. It corresponds to all the time steps of an entire month
$\sigma(t)$: Possible deviation of the forecasted building load power
$e_{forecast}$: Mean percentage of error of the neural networks
Gamma Γ: The budget of uncertainty
$\beta(P_l(t), \Gamma)$: The deviation of the forecasted load demand as a function of Γ
$z(t)$: Weight attributed to the anticipated forecasting error for each time t
$P_b(t)$: BESS power at time t in kW
$P_b^*(t)$: Optimal values for the BESS power at each time step that minimize the objective function
$P_b^{dis}(t)$: Discharging power of the BESS at time t in kW
$P_b^{ch}(t)$: Charging power of the BESS at time t in kW
P_b^{max}: Maximum power of the BESS in KW
$P_{b_{command}}(t)$: Real time BESS power command sent by the controller, in kW
η_b: Efficiency of the BESS bidirectional inverter
$y_{ch}(t)$: Binary variable conditioning the authorization of charge of the BESS
$E_b(t)$: Available energy in the BESS at the beginning of interval t
$\Delta E_b(t)$: Variation of the energy available in the BESS during the entire duration Δt which starts at time t
B_{cap} : Effective capacity of the BESS in kWh
B_{totcap} : Total capacity of the BESS in kWh
DoD: Maximum depth-of-discharge of the BESS (% 0–1)
$C_e(t)$: Cost of energy at time t in $/kWh
C_p: Cost of power in $/kW
λ_{ch}: Fee applied to the available energy in the BESS in $/kWh
$P_{p,m}$: The maximum power peak of the current month m in kW
P_c: Contract power
P_l^{max}: Maximum attainable power of the building load demand in kW
$P_l(t)$: Building load power at time t *in kW*
$\widehat{P}_l(t)$: Forecasted value of the building load power at time t in kW
$P_{setpoint}$: Power setpoint in kW sent to the real-time layer